Bioorganic & Medicinal Chemistry 19 (2011) 4473–4481

Contents lists available at ScienceDirect

Bioorganic & Medicinal Chemistry

journal homepage: www.elsevier.com/locate/bmc

Construction of dopamine sensors by using fluorescent ribonucleopeptide complexes

Fong Fong Liew [a], Tetsuya Hasegawa [a], Masatora Fukuda [a], Eiji Nakata [a], Takashi Morii [a,b,*]

[a] Institute of Advanced Energy, Kyoto University, Kyoto 611-0011, Japan
[b] CREST, JST, Uji, Kyoto 611-0011, Japan

ARTICLE INFO

Article history:
Received 25 May 2011
Revised 8 June 2011
Accepted 10 June 2011
Available online 16 June 2011

Keywords:
In vitro selection
Fluorescent sensor
Ribonucleopeptide
Dopamine
Receptor

ABSTRACT

A facile strategy of stepwise molding of a ribonucleopeptide (RNP) complex affords fluorescent RNP sensors with selective dopamine recognition. In vitro selection of a RNA-derived RNP library, a complex of the Rev peptide and its binding site Rev Responsive Element (RRE) RNA appended with random nucleotides in variable lengths, afforded RNP receptors specific for dopamine. The modular structure of the RNP receptor enables conversion of dopamine-binding RNP receptors to fluorescent dopamine sensors. Application of conditional selection schemes, such as the variation of salt concentrations and application of a counter-selection step by using a competitor ligand norepinephrine resulted in isolation of RNP receptors with defined dopamine-binding characteristics. Increasing the salt condition at the in vitro selection stage afforded RNP receptors with higher dopamine affinity, while addition of norepinephrine in the in vitro selection milieu at the counter-selection step reinforced the selectivity of RNP receptors to dopamine against norepinephrine. Thermodynamic analyses and circular dichroismic studies of the dopamine–RNP complexes suggest that the dopamine-binding RNP with higher selectivity against norepinephrine forms a pre-organized binding pocket and that the dopamine-binding RNP with higher affinity binds dopamine through the induced-fit mechanism. These results indicate that the selection condition controls the ligand-binding mechanism of RNP receptors.

1. Introduction

Fluorescent biosensors that facilitate reagent less sensitive detection of small molecules are crucial tools in the areas of therapeutics and diagnostics.[1–3] The receptor-based fluorescent sensor is a representative case of fluorescent biosensors, in which the receptor component that captures the target ligand usually sets the sensitivity and selectivity of the sensor and the signal transduction component of the sensor is responsible for converting the ligand-binding event into measurable fluorescence signals.[4–6] For generating the receptor component, in vitro selection, also known as SELEX (systematic evolution of ligands by exponential enrichment),[7–9] offers an effective strategy for generating RNA or DNA receptors (aptamers) with appropriate affinity and specificity for various targets, for which naturally occurring protein receptors are not accessible.[10–13] Modification of RNA and DNA aptamers with the fluorescence reporter component affords many RNA- and DNA-based fluorescent sensors.[14] We have reported a modular strategy for tailoring fluorescent ribonucleopeptide (RNP) sensors for ATP with a variety of binding and signal-transducing characteristics.[15,16]

A RNA-derived RNP library, in which the Rev Responsive Element (RRE) RNA appended with a randomized nucleotides region was complexed with the Rev peptide,[17,18] was applied for in vitro selection to obtain RNP receptors for various targets.[19] RNP receptors are converted into target-specific fluorescent sensors by modification of the N-terminal of the Rev peptide with various kinds of fluorophores.[16,20–22]

For the fluorescent RNP sensors to realize the selective sensing of small molecules, it is necessary to obtain RNP receptors with distinct selectivity to the target ligand. The first step of the stepwise molding of fluorescent RNP sensors, namely the in vitro selection step, controls the selectivity and affinity of the sensor for the target. The way by which the substrate was immobilized to the resin is an important parameter to control the selectivity and the affinity of RNP receptors.[23–26] It has also been reported that the conditions for the equilibrium binding of the library of molecules (RNA or DNA) to the target control the affinity and selectivity of aptamers.[27]

In this report, biologically active catecholamines are chosen as the target for the RNP receptor-based fluorescent sensor to ask a question of whether the subtle difference in the structure of small molecules could be selectively recognized by the RNP receptors and/or sensors. Catecholamines have closely related but distinct structures of the catechol ring with aliphatic chain, which is the key characteristic for each catecholamine to exert a different

* Corresponding author. Tel.: +81 774 38 3585; fax: +81 774 38 3516.
E-mail address: t-morii@iae.kyoto-u.ac.jp (T. Morii).

0968-0896/$ - see front matter © 2011 Elsevier Ltd. All rights reserved.
doi:10.1016/j.bmc.2011.06.031

receptor activation activity. Because dopamine is a valuable heuristic bridge in defective brain chemistry study over the past medical history,[28] it is of particular interest to prepare a suitable analytical tool for dopamine that will accelerate clear understanding of the relationship between the function and the structure[29] of each biologically active catecholamine. In the catecholamine biosynthesis pathway (Fig. 1), dopamine is produced by the hydroxylation of L-tyrosine followed by the decarboxylation of L-dihydoxyphenylalanine (L-dopa) by aromatic L-amino acid decarboxylase. Likewise, dopamine is the intermediate precursor of norepinephrine and epinephrine. As the further response, dopamine is converted to norepinephrine by dopamine-β-hydroxylase. Finally, phenylethanolamine *N*-methyl transferase catalyzes conversion of norepinephrine to epinephrine.[30] Each catecholamine has a distinct structure of a benzene ring with two hydroxyl groups and a terminal aminoethyl group.

In order to prepare fluorescent sensors specific for dopamine, receptors that successfully discriminate dopamine from those other catecholamine derivatives, such as norepinephrine and epinephrine, are required (Fig. 1). Previously, dopamine-binding RNA aptamers were isolated by in vitro selection[31] and its DNA homologues were reported to retain the dopamine-binding DNA activity.[32] The RNA aptamer specifically recognized the catechol group bearing 3- and 4-hydroxyl groups, but it was relatively insensitive to the modification at the aminoethyl moiety. Thus, it is an interesting challenge to design an efficient selection scheme to isolate dopamine-binding receptors with distinct specificity over L-dopa, norepinephrine and epinephrine. We report here dopamine-binding RNP receptors obtained by various in vitro selection schemes including the counter-selection and construction of fluorescent dopamine sensors through the stepwise molding strategy. We have also investigated the mechanisms by which RNP receptors recognize dopamine and demonstrated that the condition applied for the selection step governs the recognition mechanism of RNP receptors.

2. Results

2.1. Design of in vitro selection schemes for obtaining dopamine-binding ribonucleopeptides

We have combined a negative selection step using tyrosine–agarose resin at each round of the RNP selection protocol.

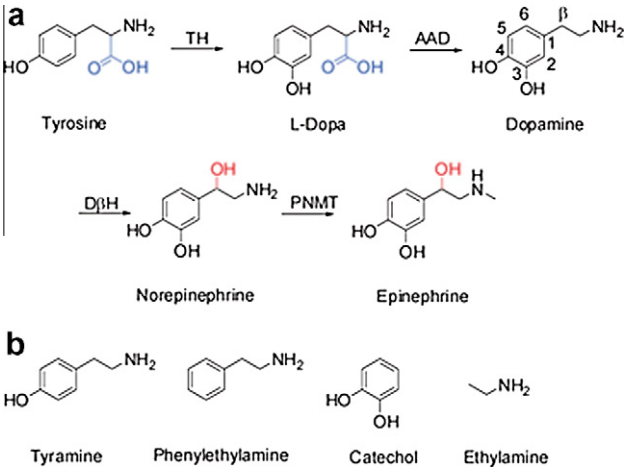

Figure 1. (a) The biosynthetic pathway for the catecholamine neurotransmitters from tyrosine. TH, tyrosine hydroxylase; AAD, aromatic L-amino acid decarboxylase; DβH, dopamine-β-hydroxylase; PNMT, phenylethanolamine methyltransferase. Dopa, 3,4-dihydroxyphenylalanine. (b) Structures of ligands bearing catecholamine-related functional groups used in this study.

Mannironi et al. selected dopamine-binding RNA aptamers at a quite high salt concentration (50 mM Tris–HCl, pH 7.4, 500 mM NaCl, and 5 mM $MgCl_2$) that would avoid nonspecific charge interactions between RNA and dopamine.[31] In vitro selection of RNP was carried out under two different NaCl concentrations 150 and 300 mM to check the effect of salt concentrations.

RNP receptors for dopamine were selected from RNP libraries (RRENn RNP library) consisting of various lengths of randomized nucleotides, ranging from 7 to 40 nucleotides.[22] The RNP library was incubated with a tyrosine-immobilized agarose resin under two different NaCl concentrations as the negative selection step. During this step, RNPs that showed affinity to the carboxyl group at the α position of the amino group would be eliminated. The flow through fraction was subjected to a second incubation with a dopamine-immobilized agarose resin at each salt condition. Unbound RNP species were extensively washed away with each binding buffer. The resin-bound RNA fractions eluted by the dopamine-containing buffer (5 mM dopamine) were collected, reverse transcribed, and applied to successive RT-PCR amplification to generate a new DNA pool. DNA templates were transcribed, and the resulting RNA was complexed with the Rev peptide to prepare an RNP pool for the next round of selection.

After 12 rounds of iterative selection and amplification at the 150 mM NaCl condition, 29 RNA clones were sequenced to reveal 16 unique sequences (designated as DL-RNP pool), which were composed of 14–37 nucleotides derived from the randomized RNA region (Fig. 2). Fourteen clones (DL02) among the 29 sequenced clones were identical, and contained a highly conserved consensus sequence 5′-CCUAUACUGACGU-3′. Two other types of consensus sequences were also identified in clones that possessed 14–37 nucleotides in the randomized region. Similarly, after 14 rounds of the selection in the condition containing 300 mM NaCl, analysis of the nucleotide sequences of 27 clones identified 21 unique sequences (designated as a DH-RNP pool), which were composed of 21–38 nucleotides derived from the randomized region (Fig. 3). DH05 and DH22 represented six and two identical clones, respectively, shared a consensus sequence 5′-UGAAAU-3′. There is no homology between the nucleotide sequences deduced from the DL- and DH-RNP pools except that DH09 RNA (Fig. 3) shows a partial similarity to DL02 RNA (Fig. 2). It turned out that each selection procedure at the different salt concentration provided unique substrate-binding RNA sequences, indicating that the specific dopamine binding by RNP is highly dependent on the salt concentration. Moreover, these consensus sequences of DL- and DH-pools showed no similarity to that of the previously reported dopamine-binding aptamers, 5′-UGUGC- - -GCACA-3′.[31]

clone	nucleotide sequences of the randomized region	nucleotide lengths
DL02	GUA **CCUAUACUG** **ACGU** CUUUU	21nt(14)
DL24	GUA **CCUAUACUG** **ACGU** CUUGU	
DL03	GUA **CCUAUACUG** **ACGU** UCUUG	
DL28	GUA **CCUAUACUG** **ACGU** UCAUA	
DL11	GUA **CCUAUACUG** **ACGU** UCAUG	
DL01	**CCUAUGCUG** CUGU CCAAUUG	20nt
DL14	GCCAGCCUU **ACGU** UCGCUAG	20nt
DL31	AUGCGGCGACCC **ACGU** CUCCUGUGUU	26nt
DL26	UGUUGUGUGCCCCUUGCU **GUUG**	22nt
DL19	UUACUUUGC **GUUG** CACUUG	19nt
DL29	AUCUGUGUAAGCU **GUUG** CACCGGUUGUAAGUAAAACU	37nt
DL23	UCCUCUAGCGAAGGAU **GUUG** UCGAACG	27nt
DL22	GUA **UUUUA** CUGCCCUC **GUUG**	20nt
DL07	UUAU **UUUUA** UAAUGUGUAUUACAUCA	26nt
DL12	AGCC **UUUUA** AUCGU	14nt
DL27	GCAUAUGACGCCUACUU	17nt

Figure 2. Nucleotide sequences obtained from the randomized region of RRENn of dopamine-binding RNP receptors after 12 rounds of in vitro selection (DL-RNP pool) with a low salt concentration buffer. The numbers in parentheses indicate the number of clone with the same nucleotide sequence. Consensus sequences were shown in bold.

clone	nucleotide sequences of the randomized region			nucleotide lengths
DH05	CACAUAUUGGUUUCAAUA	**UGGGCUGAAAU**	U	30nt (6)
DH15	GGCCACACUGACCUCGUCAU	**UGGGUUGAAAU**	GUU	34nt
DH31	GACUCUUAG	**UCGGUUGAAAU**	CGCUCCGCUGCCU	35nt
DH18	UUUCGAUA	**UGCGUUGAAUU**	UUUACAUAC	28nt
DH17	UGUCCACACCAUGCUCUGUGG	**UGGGCUGAAAU**	UGAUC	37nt
DH22	AAAUGGCUCGUUUGCGGCC	**AGGAUUGAAAU**		30nt (2)
DH34	AU	**AGGGUUGAAAC**	UCCGCCUUAAGGACAUUUU	32nt
DH36	AAUGGCUCGUUUGCGGCC	**AGGAUUGAAGU**		29nt
DH12	GG	**UGGGUUCUAAG**	CCAGCGUCCGGCUCUGUGU	33nt
DH06	AGCAUCGUAUUUUUA	**UGGCUUUAA**		24nt
DH13	GA**UGGG**UGCGC**UUGAACU**AUGAAUCU			26nt
DH19	UUUUGCGAGUCGGCUGGACAUU			22nt
DH24	AUGCAGACCGUGGUCCCCUUAGUGUUGCGAAUUUC			35nt
DH30	AUGCAGACCGUGGUCCCCUUAGUGUUGCGAAUUGC			35nt
DH04	AGCAUCAGUUUCCGCUGGCUCAA			23nt
DH20	UGAUUCGUGCUAGCCUGUUAAGAAUAAUUUUGGCCACA			38nt
DH09	GUACCUAUACUGACGUCUGAUG			22nt
DH21	UAUAUCUGCCCACUCAUCCGCUGUAUUGUGU			31nt
DH33	AAUUGGUCGUGUUGCCGGGUCUGAGGGUCCCCAUC			35nt
DH07	UUGCACCCGUUUACGCGCUUU			21nt
DH35	UGUCCAGCUGCCAGGCUUACCACCGGGCAAAGAUGCG			37nt

Figure 3. Nucleotide sequences obtained from the randomized region of RRENn of dopamine-binding RNP receptors after 14 rounds of in vitro selection (DH-RNP pool) with a high salt concentration buffer. The numbers in parentheses indicate the number of clone with the same nucleotide sequence. Consensus sequences were shown in bold.

2.2. Dopamine-binding assay of DL- and DH-RNPs based fluorescent RNP sensors

To investigate the affinity and the selectivity of isolated RNP receptors for dopamine, fluorescent RNP sensors were constructed according to the previously reported method.[15,19–22,26] The Rev peptide modified at the N-terminal with 7-methoxycoumarin-3-carboxylic acid (7mC-Rev) was complexed with DL02 RNA (DL02/7mC-Rev) and DH05 RNA (DH05/7mC-Rev), the most abundant clones in the DL- and DH-RNP pool, respectively. The relative ratio of fluorescence intensity (I/I_0) in the absence (I_0) and the presence (I) of dopamine for the fluorescent RNP complex DL02/7mC-Rev at 405 nm increased up to 2.2-fold (Fig. 4a). A nonlinear regression analysis of the titration curve yielded an equilibrium dissociation constant (K_D) of 14.9 μM for the binding complex of DL02/7mC-Rev and dopamine. Similarly, DH05/7mC-Rev showed a 1.5-fold enhancement of I/I_0 in response to the increasing concentration of dopamine (Fig. 4b). The standard binding isotherm obtained from the titration curve provided a K_D value of 4.1 μM.

The selectivity of DL02/7mC-Rev and DH05/7mC-Rev for dopamine against other catecholamine derivatives was also studied by the fluorescence titration (Fig. 4a and b). The dissociation constants for the complexes of DL02/7mC-Rev and DH05/7mC-Rev with a variety of catecholamine derivatives were obtained from the fluorescence titration curves and were summarized in Table 1. The affinity of both RNPs to tyrosine and L-dopa was much lower than that to dopamine. However, both DL02/7mC-Rev and DH05/7mC-Rev failed to discriminate dopamine from norepinephrine. Deletion of the aminoethyl group (catechol) and removal of the 3-hydroxyl group of benzene ring (tyramine) or the catechol moiety (ethylamine) resulted in complete loss of binding for DL02/7mC-Rev. The observed selectivity of DL02/7mC-Rev indicates that the catechol moiety including both the 3- and 4-hydroxyl groups and the aminoethyl group of dopamine strongly contribute to the ligand binding of DL02/7mC-Rev. Judging from the low affinity of DL02/7mC-Rev to L-dopa or tyrosine, it responded to selection pressure through tyrosine-resin elimination. Thermodynamically, the carboxyl group at the α-position of amino group was disfavored for the complex formation with DL02/7mC-Rev. The carboxyl group prevents conjugation between ligand and DL02/7mC-Rev. In contrast, DH05/7mC-Rev showed a lower sensitivity to the 3-hydroxyl group of the catechol moiety for the ligand-binding complex formation because it showed much higher affinity to tyramine as compared to DL02/7mC-Rev. DH05/7mC-Rev also showed a higher selectivity against the carboxyl group at the α-position of amino group.

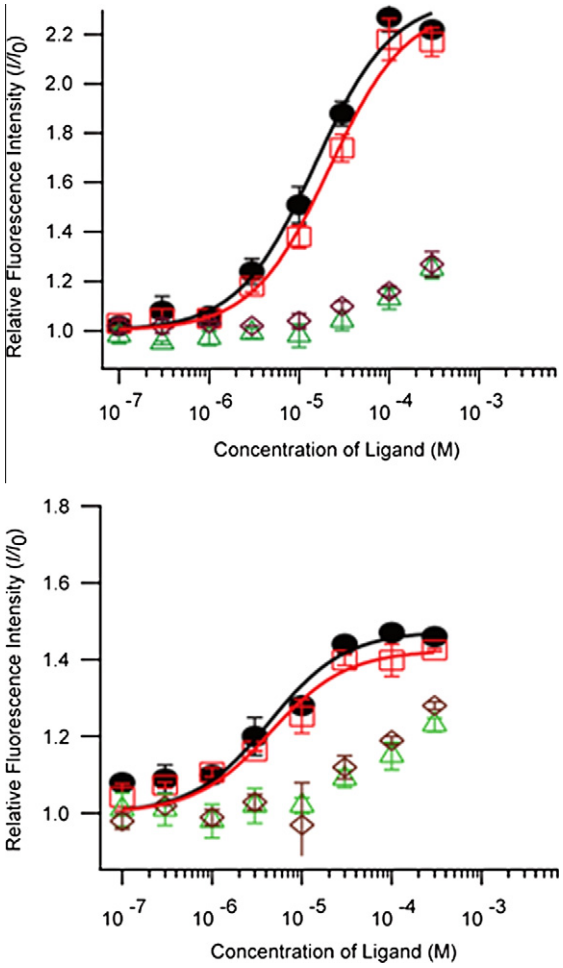

Figure 4. Titration curves for the changes of relative fluorescence intensity (I/I_0) for (a) DL02/7mC-Rev and (b) DH05/7mC-Rev with dopamine (filled black circles), norepinephrine (open red squares), L-tyrosine (open green triangles), or L-dopa (open blown diamonds).

Table 1
Equilibrium dissociation constants K_D (μM) of dopamine-binding RNP for complexes with catecholamine derivatives

Ligand	DL02	DH05	DHc25	DHc58	DHc65
Dopamine	14.9 ± 2.3	4.1 ± 1.4	60 ± 9.5	42 ± 6	3.2 ± 0.4
L-Tyrosine	>300	247 ± 33	>300	>300	>300
L-Dopa	86.4 ± 3.0	161 ± 31	>300	>300	>300
Norepinephrine	21.7 ± 3.5	6.2 ± 1.5	326 ± 28	92.4 ± 14	4.2 ± 0.4
Epinephrine	26.4 ± 4.0	14.2 ± 2.6	173 ± 28	99 ± 20	20.0 ± 6.0
Catechol	>300	>300	>300	235 ± 62	108 ± 13.2
Tyramine	>300	27 ± 5.5	>300	>280	145 ± 19.7
Ethylamine	>300	>300	>300	>300	>300
Phenylethylamine	>300	>300	>300	>300	>300

Taken together, the selection scheme including the negative selection using tyrosine-agarose resin permitted a facile preparation of dopamine-binding RNP with high selectivity for the substitution at the α-carbon of the amino group and that at the catechol moiety. DH05 RNP obtained by the selection in the presence of 300 mM NaCl showed higher affinity to dopamine than DL02 RNP obtained with 150 mM NaCl. DH05/7mC-Rev exhibited selectivity and affinity that are comparable to the previously reported RNA aptamers.[31] However, the selectivity of these RNP for the substitution at the β-carbon of the aliphatic chain remains to be improved.

2.3. Modification of the in vitro selection scheme by including a counter-selection step

We next applied a new selection scheme to isolate RNP that would discriminate dopamine against norepinephrine. The DH-RNP pool obtained after 15 rounds of in vitro selection in the presence of 300 mM NaCl was subsequently subjected to a counter-selection[33,34] by using norepinephrine as a competitive ligand, which differed from dopamine in a single hydroxyl group at the β-position of aliphatic chain (Fig. 1a). In the counter selection step, RNPs were washed off the column with a binding buffer containing norepinephrine (1 mM). The resin-bound RNPs were then specifically eluted by using a buffer containing 5 mM dopamine. After additional eight cycles of selection including the counter selection step, more convergent sequences were obtained as shown in Figure 5, designated as a DHc-RNP pool. It is noteworthy to mention that the isolated 14 clones were unique to the DHc-RNP pool and the consensus sequences 5′-AGCAU- - -GCU- -AA-3′ found in the DHc-RNP pool was completely different from that of the starting DH-RNP pool.

Each RNP from the DHc-RNP pool was subjected to a simple screening for its dopamine-binding by measuring I/I_0 of fluorescent DHc-RNPs, which were formed by the complex formation of RNA in the DHc pool with 7mC-Rev, in the absence or presence of various concentrations of dopamine (10 μM, 100 μM, 1 mM) and were summarized in Figure 6. This simple functional evaluation indicated that changes in the fluorescence signal are significant for the 7mC-Rev complexes of DHc25, DHc27, DHc43, DHc58 and DHc65. Comparison of I/I_0 values at three different dopamine concentrations (10 μM, 100 μM, 1 mM) suggests that DHc25, DHc42, DHc58 and DHc65 show high affinity to dopamine. Among the fluorescent DHc-RNPs, the dominant clone DHc25/7mC-Rev and minor clones DHc58/7mC-Rev and DHc65/7mC-Rev were selected for further analyses of their recognition mode of catecholamines.

Titration of changes of the fluorescence intensities for DHc25/7mC-Rev (Fig. 7a) with dopamine gave a K_D of 60 μM for the complex. The K_D value for the binding complex of norepinephrine was 326 μM. Comparison of the binding affinity of DHc25/7mC-Rev to other catecholamine derivatives (Table 1) revealed that DHc25/7mC-Rev, the dominant RNP in the DHc pool, had a high selectivity to the aminoethyl chain of dopamine, norepinephrine and epinephrine, and showed no detectable binding affinity to catechol, tyramine, ethylamine or phenylethylamine. Tyrosine and L-dopa were not effective substrates for DHc25/7mC-Rev. DHc58/7mC-Rev also showed selective binding to dopamine, but not as specific as DHc25/7mC-Rev (Fig. 7b, Table 2). The dopamine complex of DHc58/7mC-Rev was formed with K_D of 42 μM, while its complexes of norepinephrine and epinephrine were formed with K_D of 92 and 99 μM, respectively. Both DHc25/7mC-Rev and DHc58/7mC-Rev show binding characteristics that are different from DL02/7mC-Rev and DH05/7mC-Rev obtained from the early generation of the in vitro selection. On the other hand, the minor DHc65/7mC-Rev bounds catecholamines in the similar manner as DH05/7mC-Rev obtained from the parent DH-RNP pool (Fig. 7c, Table 2). DHc65/7mC-Rev formed stable binding complexes of dopamine and norepinephrine with K_D values of 3.2 and 4.2 μM, respectively. Both DHc25/7mC-Rev and DHc58/7mC-Rev exhibited improved binding selectivity for dopamine with the loss of binding affinity. The competitive binding condition reduced the population of RNP species that accommodate the hydroxyl group at the β-position of the aliphatic chain of norepinephrine.

Clone	nucleotide sequences of the randomized region	nucleotide lengths
DHc25	**AGCAU** GCUUUGGC **GCU** UU **AA**	20nt (15)
DHc26	**AGCAU** GGGUCUGGACCC **GCU** UA **AA**	24nt (2)
DHc27	**AGCAU** GACCUACGUC **GCU** C **AA**	21nt
DHc33	**AGCAU** CAGUUUCCGCUG **GCU** C **AA**	23nt
DHc43	**AGCAU** CGCGUGGAACACCUUUCGACUCG **GCU** UA **AA**	35nt
DHc37	**AAGUU** CAAAUUAGACCGGUCUAAUACUAAU	30nt (12)
DHc42	UUUUGAGCGUUG **AAGUU** CCUUUUGUAAAGCGGUGA	35nt
DHc47	GUGCUAAAUGCGCACUUG **AAGUU** GUUGAAUUUCUUCUA	38nt
DHc49	**AGCAU** CGCGUGGAACACCUUUCGACUCG **GCU** UA **AA**	35nt
DHc55 C	**AGCAU** CGCGUACAUCUCGGCGUACACG **GCU** UA **AA** U	36nt
DHc58	**AGCAU** CGCGUUGAACACCUUUCGACUCG **GCU** UU **AA**	35nt
DHc65	UAGUUUAGCGAUCAUCGGCGAG	22nt

Figure 5. Nucleotide sequences obtained from the randomized region of RRENn of dopamine-binding RNP receptors isolated from the additional eight rounds of counter selection using norepinephrine for DH RNA pool. The numbers in parentheses indicate the number of clone with the same nucleotide sequence. Consensus sequences were shown in bold.

2.4. Determination of thermodynamic parameters for the binding complexes of DHc RNPs and catecholamines

Possible secondary structures of the RNA subunits of selected RNP were obtained by using mfold v3.0 algorithm,[35–37] and shown in Figure S1. The overall secondary structures were calculated to maintain the secondary structure of the RRE sequence reported previously.[17] Both DHc25 and DHc58 RNPs are expected to form AU bulge and UUAA loop structures (Figs. S1a and b). These structures would provide similar binding characteristics DHc25 and DHc58 RNPs on the catecholamine recognition. The secondary structure of DHc65 RNP, the minor RNP in the DHc-RNP pool, is different from that of DHc25 or DHc58 RNP. In addition, the secondary structures suggested for DHc25, DHc58 and DHc65 RNP are quite different from the proposed secondary structures for the dopamine-binding RNA aptamers[31]

We next investigated thermodynamic parameters for the binding complexes of dopamine, norepinephrine and epinephrine with DHc25/7mC-Rev, DHc58/7mC-Rev and DHc65/7mC-Rev. The K_D values of these complexes were obtained at 4, 10, 15, 20 and 25 °C, and were shown as the van't Hoff plot (Fig. S3).[38–40] The data are fitted to the first order function of van't Hoff equation.[41] Thermodynamic parameters obtained from the van't Hoff analysis of the binding constants for DHc25/7mC-Rev, DHc58/7mC-Rev and DHc65/7mC-Rev are summarized in Table 2.

DHc25/7mC-Rev formed a dopamine-binding complex with enthalpy changes (ΔH) of −17.5 kcal mol^{-1} and unfavorable entropy changes ($-T\Delta S$) of 12.2 kcal mol^{-1} at 4 °C. Binding of norepinephrine to DHc25/7mC-Rev was due to ΔH of −13.5 kcal mol^{-1} and $-T\Delta S$ of 9.0 kcal mol^{-1}. Formation of a binding complex of DHc25/7mC-Rev and epinephrine associated with ΔH of −14.8 kcal mol^{-1} and $-T\Delta S$ of 10.0 kcal mol^{-1} (Table 2). Formation of the binding complex of DH25/7mC-Rev and catecholamine reveals that the favorable enthalpy changes for the binding of catecholamine are always offset by large unfavorable entropy changes. DHc58/7mC-Rev formed more energetically stable complexes with dopamine as compared to DHc25/7mC-Rev. Though the enthalpy changes for the dopamine complex formation of DHc58/7mC-Rev is larger than DHc25/7mC-Rev, it associates with larger unfavorable entropy changes (Table 2). Binding of catecholamines exhibited the enthalpy–entropy compensation phenomena for both DHc25/7mC-Rev and DHc58/7mC-Rev.[42] Interactions between the 4-hydroxyl group substituted aromatic ring of catecholamine with DHc25/7mC-Rev and DHc58/7mC-Rev are more critical than that between the aliphatic chain of dopamine, norepinephrine or epinephrine. Presence of the hydroxyl group at the aliphatic chain of norepinephrine reduced the enthalpy changes for the complex formation with DHc25/7mC-Rev and DHc58/7mC-Rev. The methyl group at the terminal amino group of epinephrine contributed to further reduction of the binding affinity of epinephrine. Because DHc25/7mC-Rev and DHc58/7mC-Rev reveal quite similar contributions of both enthalpy and entropy changes for the dopamine-binding complex formation, the AU bulge and the UUAA loop (Figs. S1a and b) that are common for both RNP would form the

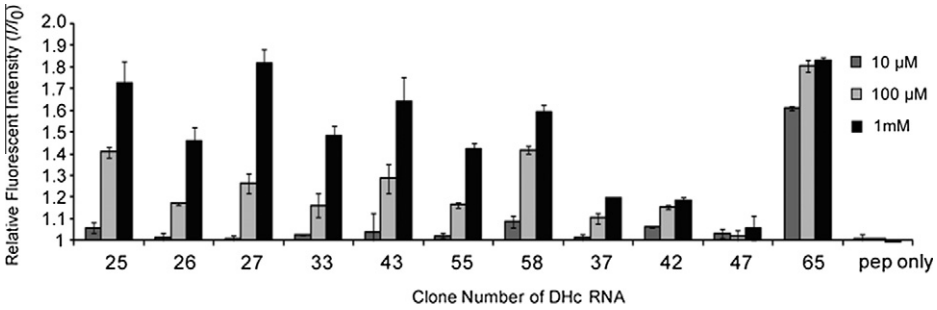

Figure 6. Changes in the relative fluorescent intensity (I/I_0) for the complexes of DHc RNAs and 7mC-Rev in the absence or presence of various concentrations (10 μM, 100 μM, 1 mM) of dopamine were evaluated at 390 nm.

binding-pocket of these RNPs. The dopamine-binding complex of DHc58/7mC-Rev exhibited a slightly higher stability than that of DHc25/7mC-Rev, which likely results from a stabilization of the putative binding site by the longer stem region adjacent to the loop. However, DHc25/7mC-Rev, the dominant RNP in the DHc-RNP pool, showed higher selectivity over norepinephrine than DHc58/7mC-Rev.

The minor RNP in the DHc-RNP pool, DHc65/7mC-Rev, showed a high affinity to dopamine but almost no specificity to norepinephrine and epinephrine. Isolation of DHc65 RNP witnesses a process of functional convergence of RNP during the selection scheme in the presence of the competitor, though the RNA sequence of DHc65 RNP does not share the consensus sequence found in the DH-RNP pool. DHc65 RNP displayed significantly different binding characteristics as compared to the other RNP from the DHc-pool, such as DHc25 and DHc58 RNP. Complex formation of DHc65/7mC-Rev with dopamine, norepinephrine or epinephrine revealed quite similar thermodynamic parameters. Both the enthalpy and entropy changes for the dopamine binding of DHc65 RNP are much larger than that of DHc25 or DHc58 RNP at 4 °C (Table 1). Though DHc65/7mC-Rev showed similar binding affinities to dopamine, norepinephrine and epinephrine, it prominently recognized both the 3- and 4-hydroxyl groups of catechol (Table 1). The observed large negative entropy changes associated with the formation of dopamine, norepinephrine and epinephrine complexes are quite similar each other, indicating that tertiary structural rearrangements for the formation of the complexes of DHc65/7mC-Rev with dopamine, norepinephrine and epinephrine take place in the similar degree. Although the number of nucleotides utilized for the ligand binding is similar for DHc65 RNP (22 nt) and DHc25 RNP (20 nt), DHc65 RNP forms the most stable dopamine–RNP complex studied here. The fact that DHc65 RNP shows a different recognition pattern from that of DHc25 RNP likely correlates to the difference in the secondary structures for these RNPs (Fig. S1).

2.5. Circular dichroismic measurements of the dopamine-binding RNPs

Solution structures of DHc RNP in absence or presence of dopamine were studied by circular dichroism (CD) measurements[43] to understand a possible correlation between the structures of RNP and their ligand-binding complexes. The CD spectra of DHc25 RNA, DHc25/7mC-Rev, and a complex of DHc25/7mC-Rev and dopamine are shown in Figure 8a. The DHc25 RNA had a strong positive band near 265 nm and a negative peak near 240 nm,[44] the characteristic feature of A-form RNA. The CD spectra of DHc25/7mC-Rev brought slight reduction in the molar ellipticity at 265 nm and a larger negative band at 220 nm, which was induced by the conformational transition of the 7mC-Rev peptide from a random to an α-helical structure upon binding to the RRE sequence. The CD spectrum of DHc25/7mC-Rev in the presence of 1 mM dopamine was almost identical to that of DHc25/7mc-Rev. Binding of dopamine to DHc25/7mC-Rev caused little or no change in the molar ellipticity at 265 nm. These results indicated that dopamine binds to a rather pre-organized binding site in DHc25 RNP. DHc58 RNP revealed almost no conformational change upon the dopamine binding. Although DHc25 RNP discriminate dopamine against norepinephrine, both the dopamine and norepinephrine complexes of DHc25 RNP revealed quite similar CD spectra (Figs. S3 and 4). This was also the case for DHc58 RNP.

In contrast, DHc65 RNP revealed a large conformational change upon its dopamine-binding complex formation (Fig. 8c). DHc65 RNA is also in the A-form structure and the formation of DHc65/7mC-Rev also induced the negative CD bands around 220 nm, assignable for the α-helix formation. Upon formation of a complex of DHc65/7mC-Rev and dopamine, a negative band was appeared at 290 nm and the positive band at 260 nm was increased. The result indicates that DHc65 RNP binds to dopamine by the induced-fit mechanism.

3. Discussion

The in vitro selection scheme including the negative selection step with tyrosine successfully reduced the population of RNP that showed affinity to tyrosine and L-dopa, the catecholamine derivatives with the carboxyl group. The high salt conditions applied in the selection step would reduce the interaction between the positively charged terminal amino group of dopamine and the negatively charged phosphate groups of RNP. In such conditions, it is expected that the complex formation of dopamine and RNP is dominantly governed by the interaction of the catechol group and the aliphatic side chain with RNP. This was born out in the present selection scheme. The in vitro selection with dopamine-bound resin at the high salt condition afforded DH05/7mC-Rev that formed a more stable dopamine-binding complex than DL02/7mC-Rev, which was obtained by in vitro selection in the low salt condition. The fluorescent RNP sensor with the high affinity to dopamine DH05/7mC-Rev showed lower selectivity to tyramine than DL02/7mC-Rev obtained from in vitro selection at the low salt condition. Thus, application of the high salt selection scheme that is expected to reduce the nonspecific ligand binding governed by the charge interaction does not always afford RNP with a higher ligand selectivity. On the other hand, the in vitro selection scheme including the counter selection step from the DHc RNP pool, where norepinephrine was utilized as the competitive ligand, resulted in isolation of RNPs that showed selectivity to dopamine over norepinephrine.

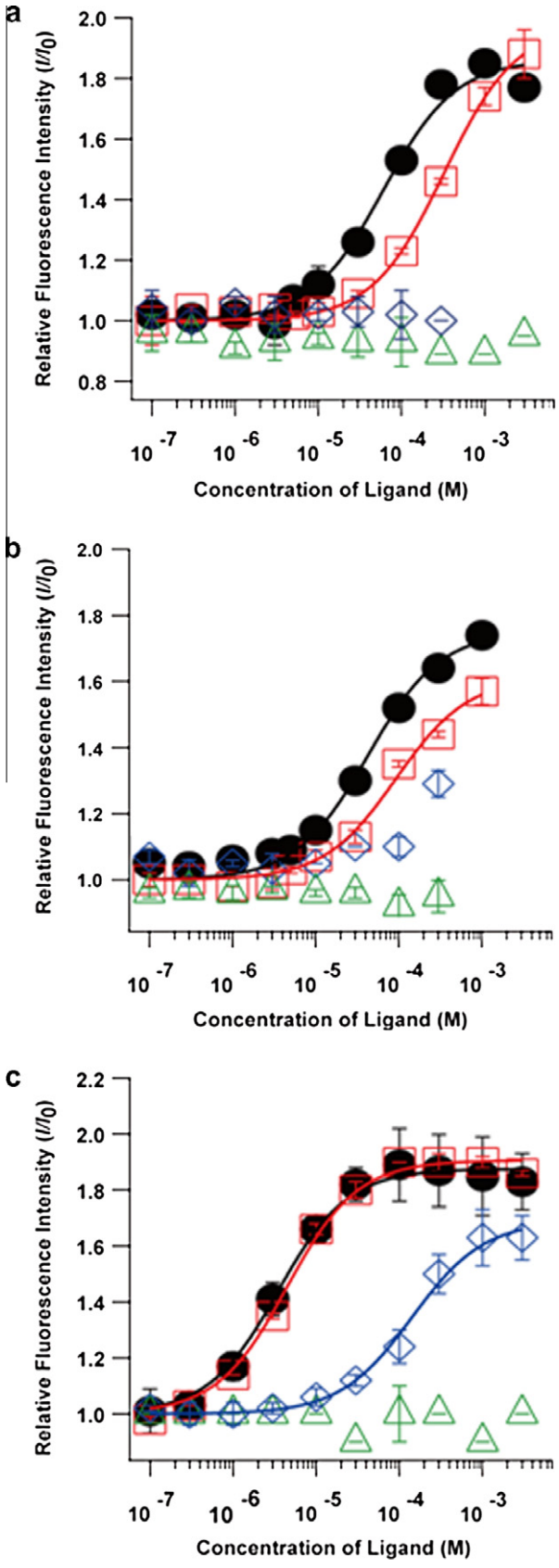

Figure 7. Saturation curves for the fluorescence emission intensity of (a) DHc25/7mC-Rev, (b) DHc58/7mC-Rev and (c) DHc65/7mC-Rev by titration with dopamine (filled black circles), norepinephrine (open red squares), L-tyrosine (open green triangles), or epinephrine (open blue diamonds).

Table 2
Thermodynamic parameters of dopamine, norepinephrine and epinephrine binding to DHc25 RNP, DHc58 RNP, and DHc65 RNP at 4 °C

DHcRNA/ 7mC-Rev	Catecholamine	ΔH (kcal mol^{-1})	$-T\Delta S$ (kcal mol^{-1})	$\Delta G_{4\ °C}$ (kcal mol^{-1})
DHc25/7mC	Dopamine	−17.5 ± 0.5	12.2 ± 0.4	−5.30 ± 0.1
	Norepinephrine	−13.5 ± 0.4	9.0 ± 0.4	−4.49 ± 0.0
	Epinephrine	−14.8 ± 0.1	10.0 ± 0.1	−4.81 ± 0.0
DHc58/7mC	Dopamine	−20.5 ± 0.0	14.7 ± 0.1	−5.75 ± 0.0
	Norepinephrine	−16.9 ± 0.2	11.8 ± 0.2	−5.05 ± 0.0
	Epinephrine	−14.8 ± 0.0	9.6 ± 0.0	−5.22 ± 0.0
DHc65/7mC	Dopamine	−24.9 ± 0.2	17.9 ± 0.3	−7.03 ± 0.1
	Norepinephrine	−24.8 ± 0.1	17.9 ± 0.1	−6.91 ± 0.1
	Epinephrine	−23.5 ± 0.2	17.0 ± 0.2	−6.51 ± 0.1

The dominant RNP in the DHc-RNP pool, DHc25/7mC-Rev, showed lower binding affinity but the higher selectivity to dopamine than DH05/7mC-Rev obtained from the parent DH-RNP pool. The obtained thermodynamic data revealed that our selection scheme against the undesired ligand attributed discrimination in the interaction of RNP with dopamine, norepinephrine and epinephrine, while the selection scheme to enhance the selectivity of RNP did not automatically produce RNP with high affinity in the present study.

CD spectral and thermodynamic data for the ligand-binding complexes of DHc25/7mC-Rev and DHc58/7mC-Rev are consistent with the pre-organized type of ligand-binding mechanism. The thermodynamic data indicates that the catechol ring is the critical recognition site for almost all the RNP selected and that the steric interference at the aliphatic chain is prone to lower the ligand-binding affinity for DHc25/7mC-Rev. DHc65/7mC-Rev forms catecholamine-binding complexes through the induced-fit mechanism, in which the equilibrium for the complex formation is often governed by faster k_{on} and k_{off} than the ligand-binding equilibrium of the pre-organized binding pocket.[45,46] In order for the selection pressure to reach the affinity maturation, RNPs with the pre-organized binding pocket have to be washed off from the bound-resin with a large excess buffer or a longer incubation time to obtain RNPs that form ligand-binding complexes governed by slower kinetics.[47–49] A selection pressure to emphasize the difference in kinetic behaviors of RNPs in the pool would be an alternative approach to obtain RNP with the high affinity and selectivity.

4. Conclusions

By applying the conditional selection scheme, we have obtained dopamine-binding RNPs with various binding characteristics and developed fluorescent RNP sensors for dopamine that show moderate selectivity against norepinephrine, and high selectivity over other catechol amines, such as epinephrine, L-dopa and tyrosine. The ligand-binding pockets are pre-organized for DHc25 and DHc58 RNP that showed similar recognition mode and binding mechanisms to dopamine. DHc25 and DHc58 RNP show higher selectivity against norepinephrine and epinephrine than DHc65 RNP, which forms a dopamine complex by the induced-fit mechanism. A selection scheme including a counter selection step by using a competitor norepinephrine afforded dopamine-binding RNPs with expected specificity. Based on the investigation of the thermodynamic parameters of the catecholamine–RNP complexes, the binding processes of catecholamines to RNP are all driven by enthalpy changes and exhibit the enthalpy–entropy compensation phenomena. Further refinements of the selection scheme, such as the kinetic control for the selection step, would realize in vitro selection of RNP with enhanced affinity and selectivity.

5. Materials and methods

Dopamine immobilized agarose resin was purchased from ICN. L-Tyrosine immobilized on cross-linked 4% beaded agarose, L-dopa, norepinephrine, epinephrine, phenylethylamine and tyrosine were purchased from Sigma–Aldrich. Catechol was purchased from Wako Chemicals. Tyramine was purchased from Tokyokasei. Klenow DNA polymerase, restriction enzyme (BamHI and EcoRI) and T4 polynucleotide kinase were purchased from New England Biolab. Gel electrophoresis grade acrylamide and bisacrylamide were obtained from Wako Chemicals. Rev peptide modified with acetic acid (Ac-Rev) and 7-methoxycoumarin-3-carboxylic acid (7mC-Rev) were synthesized as described previously.[15,19]

5.1. Nucleic acid preparations

The nucleic acids used in this study were prepared according to the procedure previously reported.[22,26] Concentrations of RNA were determined by UV spectroscopy.

5.2. In vitro selection of dopamine-binding RNP

The RRENn RNA library was prepared as previously reported[19] in the low salt buffer (100 μL) [50 mM Tris–HCl (pH 7.6), 150 mM NaCl, 0.005% Tween 20, 0.02% ascorbic acid] or in the high salt buffer (100 μL) [50 mM Tris–HCl (pH 7.6), 300 mM NaCl, 0.005% Tween 20, 0.02% ascorbic acid] by using 2 μM RNA and 3 μM Ac-Rev. Firstly, the negative selection step was carried out by using tyrosine-agarose resin (2 mM). RNP was incubated with the tyrosine-immobilized agarose resin for 30 min on ice. The RNP-bound tyrosine–agarose resin was washed three times with 300 μL of the low salt buffer. The flow-through fraction was subjected to the incubation with the dopamine–agarose resin (6 μM) in the low salt buffer. The RNP-bound resin was washed three times with 300 μL of the low salt buffer. RNP bound to the resin was eluted with the low salt buffer containing 5 mM dopamine (150 μL) for two times. RNA of the recovered RNP was precipitated with ethanol and resuspended in TE buffer (50 μL). After reverse transcription with AMV (Avian Myeloblastosis Virus) reverse transcriptase (Promega) of the selected RNA using the 3′-DNA primer used in PCR amplification and successive PCR amplification (RT-PCR) using the 5′- and 3′-DNA primer, DNA templates were transcribed and the resulting RNAs were subjected to the next round of selection. After 12 rounds of low salt buffer selection, collected RNP pool was designated as the DL-RNP pool. In vitro selection in the high salt buffer was carried out in the similar manner for 14 rounds of selection to give the DH-RNP pool.

5.3. Counter selection of dopamine binding ribonucleopeptide with presence of norepinephrine (RNA/Rev)

The DH-RNP pool obtained from the high salt condition was subjected to another eight rounds of selection by using an equilibrium binding buffer (100 μL) containing 50 mM Tris–HCl (pH 7.6), 300 mM NaCl, 0.005% Tween 20, 0.02% ascorbic acid, 1 mM norepinephrine and the RRENn RNP library (2 μM RNA and 3 μM Ac-Rev). RNP and the dopamine-immobilized agarose resin (6 μM) were incubated on ice for 30 min. The resin was washed three times with a buffer (300 μL) containing 50 mM Tris–HCl (pH 7.6), 300 mM NaCl and 5 mM $MgCl_2$. The resin-bound RNPs were eluted twice by the high salt buffer containing 5 mM dopamine. RNA of the recovered RNP was precipitated with ethanol and resuspended in TE buffer (50 μL). After reverse transcription with AMV reverse transcriptase (Promega) of the selected RNA using the 3′-DNA primer used in PCR amplification and successive PCR amplification (RT-PCR) using the 5′- and 3′-DNA primer, DNA templates were transcribed and the resulting RNAs were subjected to the next round of selection.

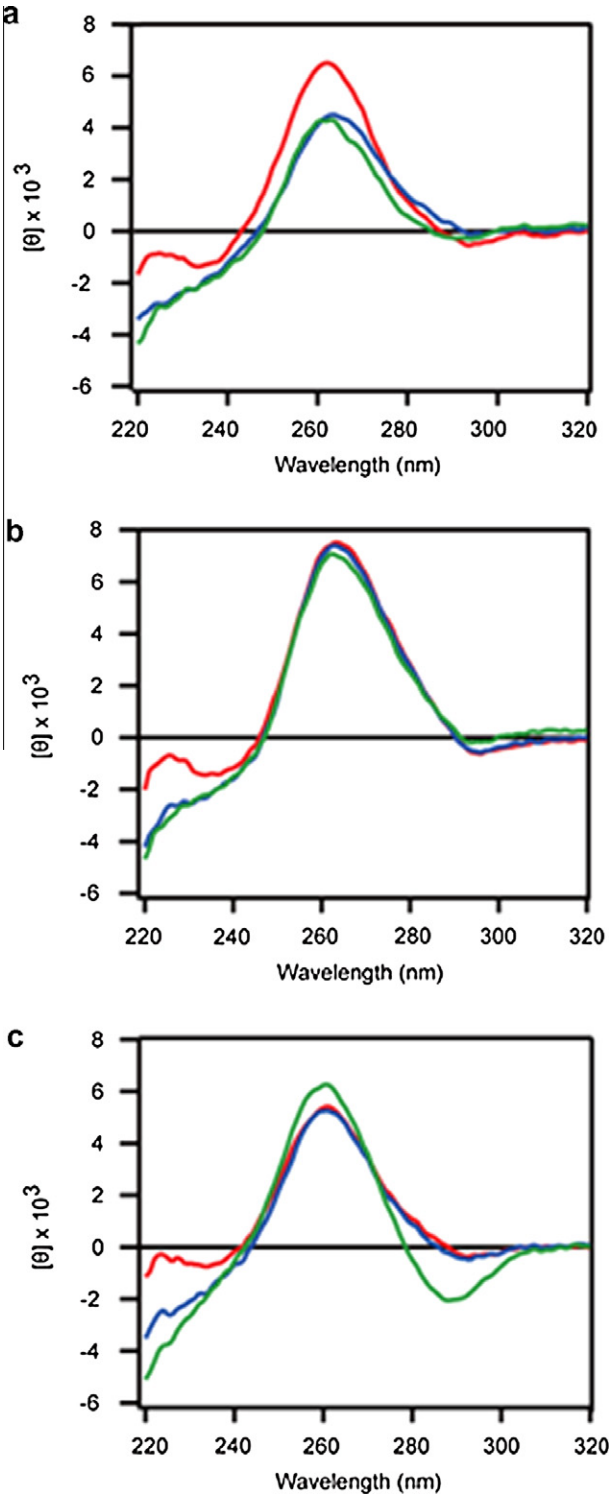

Figure 8. The CD spectra of (a) DHc25, (b) DHc58 and (c) DHc65. RNA only (red line), RNP only (blue line), and RNP with dopamine (green line) spectra were shown, respectively.

5.4. Sequencing analysis of selected RNA

Selected RNA pools were converted to DNA and PCR-amplified to introduce BamHI and EcoRI restriction sites by using primers

5′-GCGGGATCCTTTCGGCCTGTACCGTCA-3′ and 5′ CGGAATTCTAATACGACTCACTATAGG-3′. After enzymatic digestions, DNAs were cloned into the pUC 19 vector using Ligation Kit ver 2 (TaKaRa) and sequenced using a BigDye Terminator Cycle Sequencing Kit (Applied Biosystems) with a model 377 DNA sequencer (Applied Biosystems)

5.5. Fluorescence measurements on the microplate

The 96-well fluorescence measurements were performed on a Wallac ARVOsx 1420 multilabel counter. The binding assay was evaluated by using the following conditions: 1 μM RNA and 1 μM 7mC-Rev in 50 mM Tris–HCl (pH 7.6), 5 mM $MgCl_2$, 0.005% Tween 20 and 0.02% ascorbic acid with 150 mM NaCl (DL-RNP) or with 300 mM NaCl (DH or DHc-RNP). Well-mixed samples with different concentration of the ligands bearing catecholamine-related functional groups were incubated at 4 °C for 20 min, then emission spectra were measured (λ_{ex} = 355 nm, λ_{em} = 390 nm).

$$F_{obs} = A(([RNP]_T + [substrate]_T + K_D) - (([RNP]_T + [substrate]_T + K_D)^2 - (4[RNP]_T[substrate]_T)^{1/2})/2[RNP]_T)$$

where A is the increase in fluorescence at saturating substrate concentrations ($F_{max}-F_{min}$), K_D is the equilibrium dissociation constant, and $[RNP]_T$ and $[substrate]_T$ are the total concentrations of RNP and the substrate, respectively.

5.6. RNA secondary structure prediction

Prediction of the secondary structure of DHc25 RNA, DHc 58 RNA and DHc 65 RNA by using Mfold v3.0 algorithm (offered at http://mfold.rna.albany.edu/). Folding was done at 37 °C with 1 M NaCl, specifying that the RRE region is in the reported secondary structure.[35–37]

5.7. Thermodynamic parameter of the RNP-ligand binding complexes

RNP (0.5 μM RNA: 0.5 μM 7mC-Rev) samples in binding buffer 50 mM Tris–HCl (pH 7.6), 300 mM NaCl, 5 mM $MgCl_2$, 0.005% Tween 20, 0.02% ascorbic acid with different concentration of catecholamine were prepared. Samples after well-mixed were incubated at different temperature: 4, 10, 15, 20 and 25 °C for 20 min. Fluorescent intensity of samples was measured (λ_{ex} = 355 nm, λ_{em} = 390 nm) by using Hitachi F7000 fluorescent spectrophotometer.

Through plot of ln $1/K_D$ against 1/Temperature (Kelvin), both ΔH^θ and ΔS^θ were extracted. Consequently, the changes in Gibbs free energy were calculated by the following formula[50] (T = 298 K and R = 8.314 J K^{-1} mol^{-1}).

$$\ln 1/K_D = -\Delta H^\theta/RT + \Delta S^\theta/R \quad (1)$$

$$-T\Delta S^\theta = \Delta G^\theta - \Delta H^\theta \quad (2)$$

5.8. Circular dichroism spectroscopy measurements

Circular dichroism spectra were recorded on a Jasco J-725J spectropolarimeter (Jasco, Inc., Easton, MD) interfaced with a computer and equipped with a heating/cooling device and nitrogen purging facilities. The CD spectrum of 3 μM DHc RNA, and 3 μM DHc RNP (ratio of RNA: 7mC-Rev = 1:4) complex with dopamine [1 mM or 50 μM (DHc 65)], norepinephrine [1 mM or 50 μM (DHc 65)] or epinephrine [1 mM or 50 μM (DHc 65)] were measured in 50 mM Tris–HCl (pH 7.6), 300 mM NaCl, 5 mM $MgCl_2$, 0.005% Tween 20, and 0.02% ascorbic acid at 4 °C. The data were gathered at the average of 10 time scans (scanning rate of 100 nm min^{-1}) from 320 to 190 nm. The data were collected in units of millidegrees versus wavelength.

Acknowledgment

This work was supported in part by the Grants-in-Aid for Scientific Research from the Ministry of Education, Culture, Sports, Science and Technology, Japan to T.M. (No. 20241051).

Supplementary data

Supplementary data (thermodynamic parameters of fluorescent RNP to dopamine, norepinephrine and epinephrine at 4 °C (Table S1), possible secondary structures of DHc25 RNA, DHc58 RNA and DHc65 RNA obtained by mfold v3.2 algorithm. (Fig. S1), saturation curves for the fluorescence emission intensity of fluorescent RNP to all ligands used in this study (Fig. S2), the van't Hoff analysis (Fig. S3) and CD spectra of the RNP complexes with catecholamine-related ligands (Fig. S4)) associated with this article can be found, in the online version, at doi:10.1016/j.bmc.2011.06.031.

References and notes

1. Johnsson, N.; Johnsson, K. *ACS Chem. Biol.* **2007**, *2*, 31.
2. Wang, H.; Nakata, E.; Hamachi, I. *ChemBioChem* **2009**, *10*, 2560.
3. Tainaka, K.; Sakaguchi, R.; Hayashi, H.; Nakano, S.; Liew, F. F.; Morii, T. *Sensors* **2010**, 1355.
4. Zhang, J.; Campbell, R. E.; Ting, A. Y.; Tsien, R. Y. *Nat. Rev. Mol. Cell Biol.* **2002**, 906.
5. Liu, J.; Cao, Z.; Lu, Y. *Chem. Rev.* **2009**, *109*, 1948.
6. Helinga, H. W.; Marvin, J. S. *Trends Biotechnol.* **1998**, *16*, 183.
7. Tuerk, C.; Gold, L. *Science* **1990**, *249*, 505.
8. Guo, K. T.; Paul, A.; Schichor, C.; Ziemer, G.; Wendel, H. P. *Int. J. Mol. Sci.* **2008**, *9*, 668.
9. Sefah, K.; Shangguan, D.; Xiong, X.; O'Donoghue, M. B.; Tan, W. *Nat. Protoc.* **2010**, *5*, 1169.
10. Ellington, A. D.; Szostak, J. W. *Nature* **1990**, *346*, 818.
11. Osborne, S. E.; Ellington, A. D. *Chem. Rev.* **1997**, *97*, 349.
12. Wilson, D. S.; Szostak, J. W. *Annu. Rev. Biochem.* **1999**, *68*, 611.
13. Famulok, M.; Hartig, J. S.; Mayer, G. *Chem. Rev.* **2007**, *107*, 3715.
14. Cho, E. J.; Lee, J.-W.; Ellington, A. D. *Annu. Rev. Anal. Chem.* **2009**, *2*, 241.
15. Hagihara, M.; Fukuda, M.; Hasegawa, T.; Morii, T. *J. Am. Chem. Soc.* **2006**, *128*, 12932.
16. Hasegawa, T.; Hagihara, M.; Fukuda, M.; Morii, T. *Nucleosides Nucleotides Nucleic acids* **2007**, *26*, 1277.
17. Battiste, J. L.; Mao, H.; Rao, N. S.; Tan, R.; Muhandiram, D. R.; Kay, L. E.; Frankel, A. D.; Williamson, J. R. *Science* **1996**, *273*, 1547.
18. Sato, S.; Fukuda, M.; Hagihara, M.; Tanabe, Y.; Ohkubo, K.; Morii, T. *J. Am. Chem. Soc.* **2005**, *127*, 30.
19. Morii, T.; Hagihara, M.; Sato, S.; Makino, K. *J. Am. Chem. Soc.* **2002**, *124*, 4617.
20. Fukuda, M.; Hayashi, H.; Hasegawa, T.; Morii, T. *Trans. Mat. Res. Soc. Jpn.* **2009**, *34*, 525.
21. Hasegawa, T.; Ohkubo, K.; Yoshikawa, S.; Morii, T. *J. Surf. Sci. Nanotech.* **2005**, *3*, 33.
22. Hasegawa, T.; Hagihara, M.; Fukuda, M.; Nakano, S.; Fujieda, N.; Morii, T. *J. Am. Chem. Soc.* **2008**, *130*, 8804.
23. Sassanfar, M.; Szostak, J. W. *Nature* **1993**, *364*, 550.
24. Burke, D. H.; Gold, L. *Nucleic Acids Res.* **1997**, *25*, 2020.
25. Weill, L.; Louis, D.; Sargueil, B. *Nucleic Acids Res.* **2004**, *32*, 5045.
26. Nakano, S.; Mashima, T.; Matsugami, A.; Inoue, M.; Katahira, M.; Morii, T. *J. Am. Chem. Soc.* **2011**, *133*, 4567.
27. Stoltenburg, R.; Reinemann, C.; Strehlitz, B. *Biomol. Eng.* **2007**, *24*, 381.
28. Björklund, A.; Dunnett, S. B. *Trends Neurosci.* **2007**, *30*, 194.
29. Villoslada, P.; Oksenberg, J. R. *Future Neurol.* **2006**, *1*, 159.
30. Flatmark, T. *Acta Physiol Scand* **2000**, *168*, 1.
31. Mannironi, C.; Nardo, A. D.; Fruscoloni, P.; Tocchini-Valentini, G. P. *Biochemistry* **1997**, *36*, 9726.
32. Walsh, R.; DeRosa, M. C. *Biochem. Biophys. Res. Commun.* **2009**, *388*, 732.
33. Jenison, R. D.; Gill, S. C.; Pardi, A.; Polisky, B. *Science* **1994**, *263*, 1425.
34. Haller, A. A.; Sarnow, P. *Proc. Natl. Acad. Sci. U.S.A.* **1997**, *94*, 8521.
35. Zuker, M. *Science* **1989**, *244*, 48.
36. Mathew, D. H.; Sabina, J. K.; Zuker, M.; Turner, D. H. *J. Mol. Biol.* **1999**, *288*, 911.
37. Zuker, M. *Nucleic Acids Res.* **2003**, *31*, 3406.
38. Kumar, N.; Maiti, S. *Biochem. Biophys. Res. Commun.* **2004**, *319*, 759.
39. André, C.; Xicluna, A.; Guillaume, Y. *Electrophoresis* **2005**, *26*, 3247.
40. Lin, P.-H.; Yen, S.-L.; Lin, M.-S.; Chang, Y.; Lousi, S. R.; Higuchi, A.; Chen, W.-Y. *J. Phys. Chem. B* **2008**, *112*, 6665.

41. Borea, P. A.; Dalpiaz, A.; Varani, K.; Gilli, K.; Gilli, G. *Biochem. Pharmacol.* **2000**, *60*, 1549.
42. Shiroshi, M.; Yokota, A.; Tsumoto, K.; Kondo, H.; Nishimiya, Y.; Horii, K.; Matsushima, M.; Ogasahara, K.; Yutani, K.; Kumagai, I. *J. Biol. Chem.* **2001**, *276*, 23042.
43. Serin, G.; Joseph, G.; Ghisolfi, L.; Bauzan, M.; Erard, M.; Amalric, F.; Bouvet, P. *J. Biol.Chem.* **1997**, *272*, 13109.
44. Loret, E. P.; Georgel, P.; Johnson, W. C., Jr.; Ho, P. S. *Proc. Natl. Acad. Sci. U.S.A.* **1992**, *89*, 9734.
45. Karbstein, K.; Herschlag, D. *Proc. Natl. Acad. Sci. U.S.A.* **2003**, *4*, 2300.
46. Drabovich, A. P.; Berezovski, M.; Okhonin, V.; Krylov, S. *Anal. Chem.* **2006**, *78*, 3171.
47. Zhou, H. *Biophys. J.* **2010**, *98*, L15–L17.
48. Gao, J.; Sidhu, S.; Wells, J. A. *Proc. Natl. Acad. Sci. U.S.A.* **2009**, *106*, 3071.
49. Zahnd, C.; Sarkat, C. A.; Plückthun, A. *Protein Eng. Des. Sel.* **2010**, *23*, 175.
50. Chaires, J. B. *Annu. Rev. Biophys.* **2008**, *37*, 135.